Environmental Science & Technology

Article

pubs.acs.org/est

Using Mercury Isotopes To Understand Mercury Accumulation in the Montane Forest Floor of the Eastern Tibetan Plateau

Xun Wang,[†,‡] Ji Luo,[§] Runsheng Yin,[∥,⊥] Wei Yuan,[†,‡] Che-Jen Lin,[†,#] Jonas Sommar,[†] Xinbin Feng,*[,†] Haiming Wang,[§] and Cynthia Lin[▽]

[†]State Key Laboratory of Environmental Geochemistry, Institute of Geochemistry, Chinese Academy of Sciences, Guiyang 550081, China

[‡]University of Chinese Academy of Sciences, Beijing 100049, China

[§]Key Laboratory of Mountain Surface Processes and Ecological Regulation, Institute of Mountain Hazards and Environment, Chinese Academy of Sciences, and Ministry of Water Conservancy, Chengdu 610041, China

[∥]State Key Laboratory of Ore Deposit Geochemistry, Institute of Geochemistry, Chinese Academy of Sciences, Guiyang 550081, China

[⊥]Environmental Chemistry and Technology Program, University of Wisconsin-Madison, Madison, Wisconsin 53706, United States

[#]Center for Advances in Water and Air Quality, Lamar University, Beaumont, Texas 77710, United States

[▽]The McKetta Department of Chemical Engineering, University of Texas at Austin, Austin, Texas 78712, United States

Supporting Information

ABSTRACT: Mercury accumulation in montane forested areas plays an important role in global Hg cycling. In this study, we measured stable Hg isotopes in soil and litter samples to understand Hg accumulation on the forest floor along the eastern fringe of the Tibetan Plateau (TP). The low atmospheric Hg inputs lead to the small Hg pool size (23 ± 9 mg m^{-2} in 0−60 cm soil horizon), up to 1 order of magnitude lower than those found at sites in Southwest China, North America, and Europe. The slightly negative Δ^{199}Hg (−0.12 to −0.05‰) in the litter at low elevations (3100 to 3600 m) suggests an influence of local anthropogenic emissions, whereas the more significant negative Δ^{199}Hg (−0.38 to −0.15‰) at high elevations (3700 to 4300 m) indicates impact from long-range transport. Hg input from litter is more important than wet deposition to Hg accumulation on the forest floor, as evidenced by the negative Δ^{199}Hg found in the surface soil samples. Correlation analyses of Δ^{199}Hg versus total carbon and leaf area index suggest that litter biomass production is a predominant factor in atmospheric Hg inputs to the forest floor. Precipitation and temperature show indirect effects on Hg accumulation by influencing litter biomass production in the eastern TP.

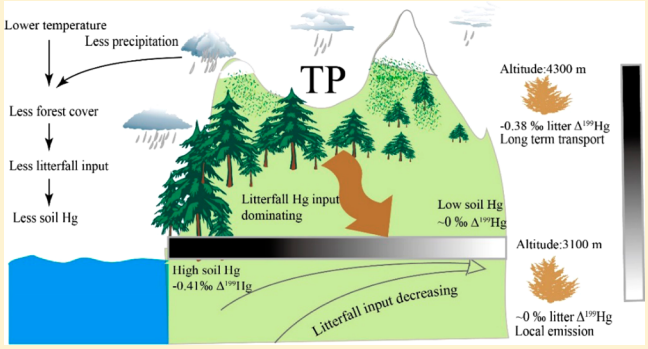

1. INTRODUCTION

Elevated atmospheric mercury deposition to pristine ecosystems is a persisting environmental issue.[1−3] Remote mountain forests represent a class of pristine ecosystems that have a landscape at an elevation of 2500 m above sea level (a.s.l.) or higher, or at an elevation of 300−2500 m with sharp changes in elevation within a short distance.[4] Such forests account for 20% of the total global forested area.[4] There is growing evidence for augmented atmospheric Hg deposition at high-elevation sites, and montane areas act as convergence zones for atmospheric Hg.[5,6] Enriched Hg concentrations in soil,[6] vegetation, precipitation, and wildlife (e.g., birds, salamanders, etc.)[7] have been reported in montane areas. However, because of biological, orographic, and climatic influences, the biogeochemical cycling of Hg in montane ecosystems remains unclear.[6,8]

The Tibetan Plateau (TP), with an average elevation of >4000 m a.s.l., is the "Third Pole" on earth. The TP has a remote location and low population density. However, anthropogenic influences have become more and more pronounced over past three decades. Industrialization in South and East Asia has accelerated the loading of Hg to the TP.[9−11] The Hg concentration in the forest floor has increased by a factor of 2 to 3 since the 1980s.[10,12,13] Hg accumulated in the soil can be methylated through microbial and abiotic processes.[14,15] The produced methylmercury (MeHg) has a

Received: July 29, 2016
Revised: December 2, 2016
Accepted: December 13, 2016
Published: December 13, 2016

DOI: 10.1021/acs.est.6b03806
Environ. Sci. Technol. 2017, 51, 801−809

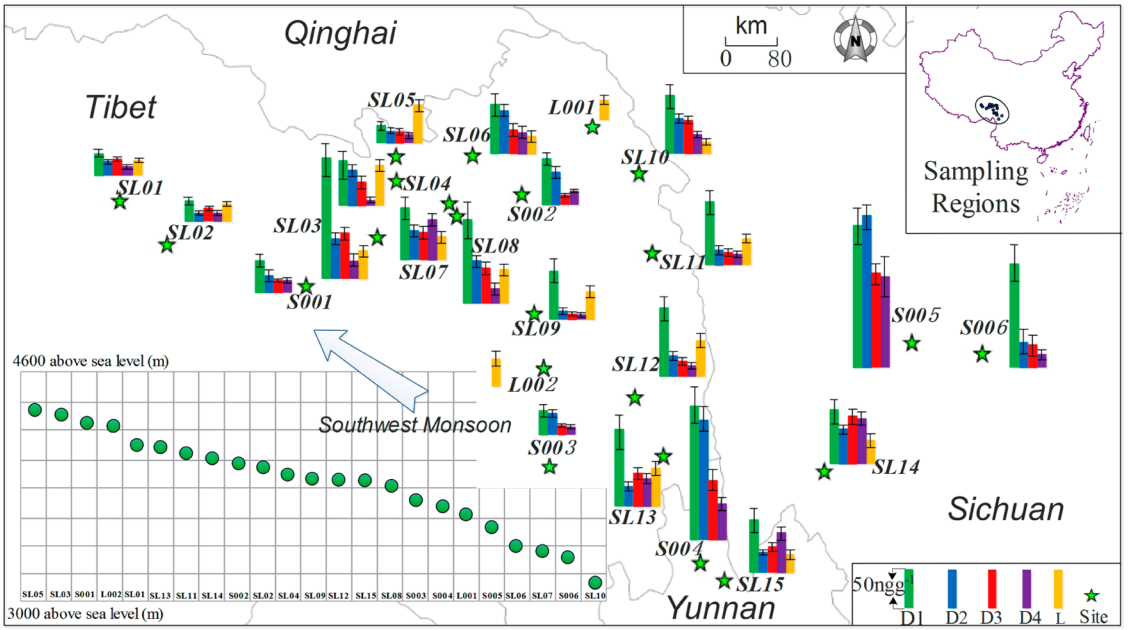

Figure 1. Hg concentrations in litter (L), 0−8 cm surface soil (D1), 8−20 cm soil (D2), 20−30 cm soil (D3), and 30−60 cm soil (D4) for each sampling site.

strong bioaccumulation capability, can be transported to aquatic ecosystems via surface runoff, and leads to contamination in aquatic food webs of the TP.[8,16−18] As a result, the source, deposition, and accumulation of Hg in the forests of the TP need to be better understood.

Stable Hg isotopes are useful tracers to understand the sources and fate of Hg in the environment. Hg isotopes can undergo mass-dependent fractionation (MDF) and mass-independent fractionation (MIF) during geochemical cycling of Hg.[19−22] Photochemical reactions are associated with both MDF and MIF of Hg, whereas biotic and dark abiotic reactions display Hg MDF without significant Hg MIF.[20,23,24] Isotopic ratios such as $\Delta^{199}Hg/\Delta^{201}Hg$ and $\Delta^{199}Hg/\Delta^{202}Hg$ have been applied to diagnose specific processes.[19,20,23,24] Hg isotopic composition offers insights into the geochemical cycling of Hg (e.g., deposition, accumulation, and re-emission) in the forest ecosystem.[23,25,26] Distinct Hg isotope signatures have been documented in foliage, rainwater, forest soil, and bedrocks.[20,24] The Hg MIF signature is particularly useful to differentiate Hg inputs from atmospheric depositions and rock weathering.[23,25,27]

In this study, we investigated the isotope composition of Hg in leaf litter and soil profiles. We aimed to identify the sources of Hg in leaf litter and the inputs of atmospheric Hg to the TP forest floor. The implications in terms of Hg accumulation in the TP forests are discussed.

2. EXPERIMENTAL SECTION

2.1. Sample Collection. Details of the study area, sample sites, and sample collection have been described previously.[12,28−30] Briefly, 23 timberline forest sites in the eastern TP (30.3−31.6° N, 94.2−98.6° E; Figure 1 and Table S1) were selected, having elevation ranges of 3100 to 4300 m a.s.l. The dominant tree species of the studied area is *Picea crassifolia*, and the soil is mainly Luvisol. The studied area is influenced by the southwestern monsoon, and annual air temperatures and annual precipitation are 3−5 °C and 400−700 mm, respectively.[30,31]

We collected both soil and litter samples at 15 of the 23 forest sites (SL01−SL15), litter samples only at sites L001 and L002, and soil samples only at sites S001−S006 (Figure 1). To minimize potential seasonal influences, all of the samples were collected from July to August 2012. At each site, three 20 m × 30 m plots were established for sample collection. Each plot contained 24 subplots (5 m × 5 m). Fresh litter from 12 subplots of each plot was randomly sampled and mixed as one composite sample. The leaf area index (LAI) of each subplot was measured using an LAI-2200 instrument.[32] Similar sampling schemes were applied for 0−8 cm surface soil, 8−20 cm soil, 20−30 cm soil, and 30−60 cm soil. The sample pretreatment is discussed in detail in the Supporting Information (SI).

2.2. Measurements. Hg concentrations of the samples were measured by a Lumex RA-915+ Hg analyzer.[33] Total carbon (C) was measured by an Vario Macro Cube C analyzer (Elementar, Langenselbold, Germany; limit of detection ≤10 ppm; discussed in detail in the SI).[33] The soil bulk density was measured using the methodology described by Maynard and Curran.[34] The Hg pool size in each horizon was estimated as

$$P_i = Hg_i \times B_i \times T_i \times (1 - F_i) \quad (1)$$

where P_i is the soil Hg pool, Hg_i is the soil Hg concentration, T_i is the horizon thickness, B_i is the soil bulk density, and F_i is the fraction of coarse fragment by volume (%).

Prior to Hg isotope measurements, all of the litter and soil samples were processed by a double-stage tube furnace (discussed in detail in the SI),[35] allowing for complete oxidation of organic substances and thermal reduction of Hg^{II}. MDF is reported in δ notation using the unit of per mil (‰) referenced to the NIST-3133 Hg standard solution:

$$\delta^{202}Hg(‰) = 1000 \times \left[\frac{(^{202}Hg/^{198}Hg)_{sample}}{(^{202}Hg/^{198}Hg)_{NIST\text{-}3133}} - 1 \right] \quad (2)$$

DOI: 10.1021/acs.est.6b03806
Environ. Sci. Technol. 2017, 51, 801−809

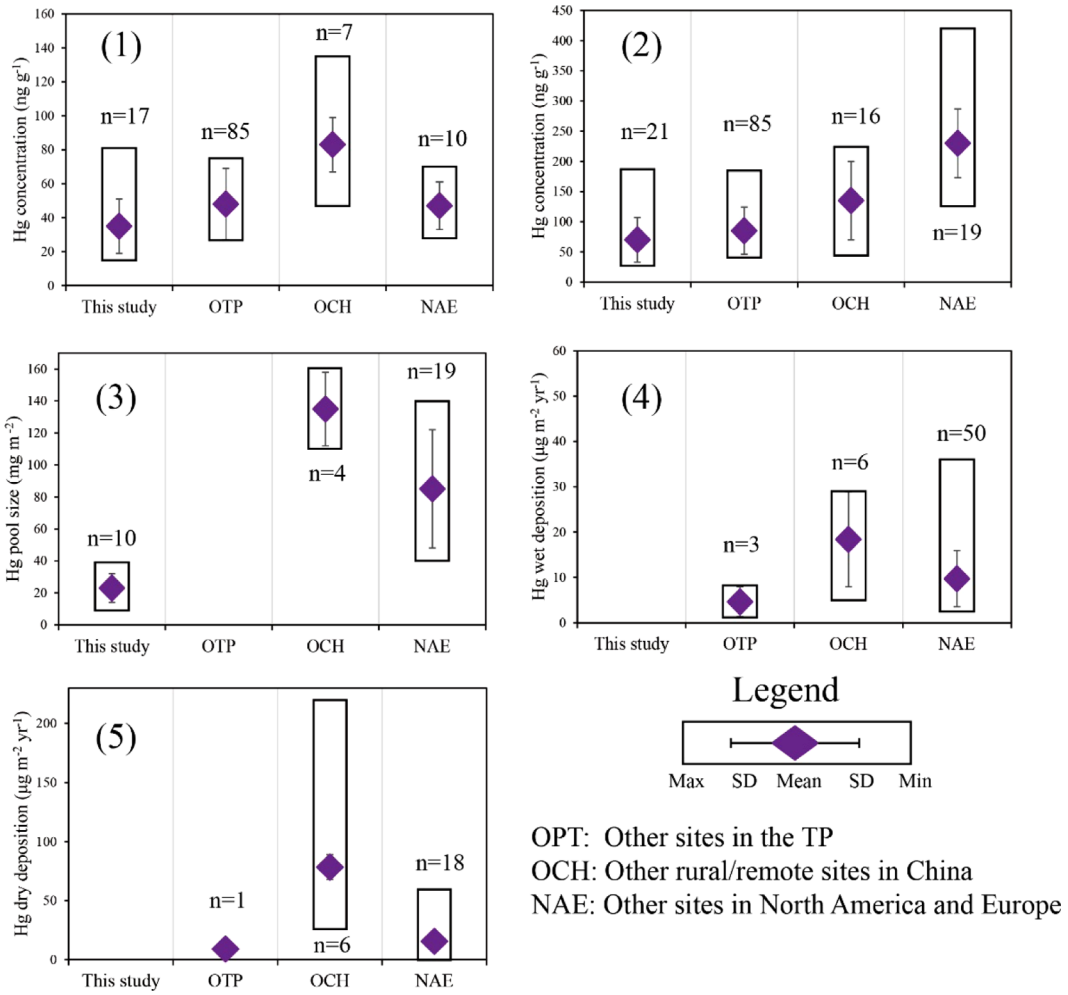

Figure 2. Differences in (1) Hg concentration of litter, (2) Hg concentration of surface soil, (3) Hg pool size of the 0−60 cm soil horizon, (4) Hg wet deposition, and (5) Hg deposition through litter between this study and documented forests.[5,10,11,13,33,37−54]

MIF is reported as Δ^nHg (n = 199, 200, 201) in per mil (‰) and was calculated following the convention suggested by Blum and Bergquist:[19]

$$\Delta^{199}\mathrm{Hg}(‰) = \delta^{199}\mathrm{Hg} - 0.2520 \times \delta^{202}\mathrm{Hg} \quad (3)$$

$$\Delta^{200}\mathrm{Hg}(‰) = \delta^{200}\mathrm{Hg} - 0.5024 \times \delta^{202}\mathrm{Hg} \quad (4)$$

$$\Delta^{201}\mathrm{Hg}(‰) = \delta^{201}\mathrm{Hg} - 0.7520 \times \delta^{202}\mathrm{Hg} \quad (5)$$

The reproducibility of the Hg isotopic data was assessed by measuring replicate sample solutions. UM-Almadén secondary standard solution was analyzed for every 10 samples. The acid matrices and Hg concentrations of NIST-3133 and bracketed samples were matched. The results of UM-Almadén (mean ± standard deviation (SD): δ^{202}Hg = −0.53 ± 0.04‰; Δ^{199}Hg = −0.00 ± 0.04‰; Δ^{201}Hg = −0.03 ± 0.02‰; n = 16) and BCR-482 (δ^{202}Hg = −1.67 ± 0.08‰; Δ^{199}Hg = −0.57 ± 0.05‰; Δ^{201}Hg = −0.58 ± 0.04‰; n = 7) are consistent with previous studies.[19,36]

3. RESULTS AND DISCUSSION

3.1. Hg Concentration and Soil Hg Pool Size. The Hg concentrations for all of the samples are shown in Figure 1. The Hg concentration in litter ranges from 15 to 81 ng g^{-1}, with a mean value of 35 ± 16 ng g^{-1} (n = 17). For the soil samples, 0−8 cm soil (surface soil) has the highest Hg concentration (mean = 70 ± 37 ng g^{-1}, n = 21), followed by 8−20 cm soil (35 ± 16 ng g^{-1}, n = 21), 20−30 cm soil (34 ± 16 ng g^{-1}, n = 21), and 30−60 cm soil (26 ± 18 ng g^{-1}, n = 21). In addition, the soil Hg pool size (Figure S1) is 4.6 ± 1.8 mg m^{-2} for 0−8 cm soil (n = 15), 3.7 ± 2.1 mg m^{-2} for 8−20 cm soil (n = 15), 4.4 ± 2.5 mg m^{-2} for 20−30 cm soil (n = 15), and 8.9 ± 5.8 mg m^{-2} for 30−60 cm soil (n = 15).

Figure 2 shows the differences in Hg concentration, Hg pool size, and Hg deposition influx between the TP and other forests worldwide.[5,10,11,13,33,37−54] For the Hg concentration in litter, the data are comparable to values reported in other TP forests (t test, P = 0.67) and in conifer forests from Europe and North America (P = 0.49; Figure 2.1) but significantly lower than values reported in rural sites of China (P = 0.00; Figure 2.1). The Hg concentration in 0−8 cm soil is comparable to that of the surface soil of the other TP forests (P = 0.65; Figure 2.2) but lower than that of the surface soil in rural forests of China (P = 0.01; Figure 2.2) and North America and Europe (P = 0.02; Figure 2.2). The Hg pool sizes in this study are lower than those reported for 0−60 cm soil in China, North America, and Europe (P = 0.01; Figure 2.3). Our sampling sites are mature forest sites. The relatively low surface Hg concentration and low soil Hg pool size are attributed to lower Hg deposition influxes over the TP. This is consistent with earlier observations

DOI: 10.1021/acs.est.6b03806
Environ. Sci. Technol. 2017, 51, 801−809

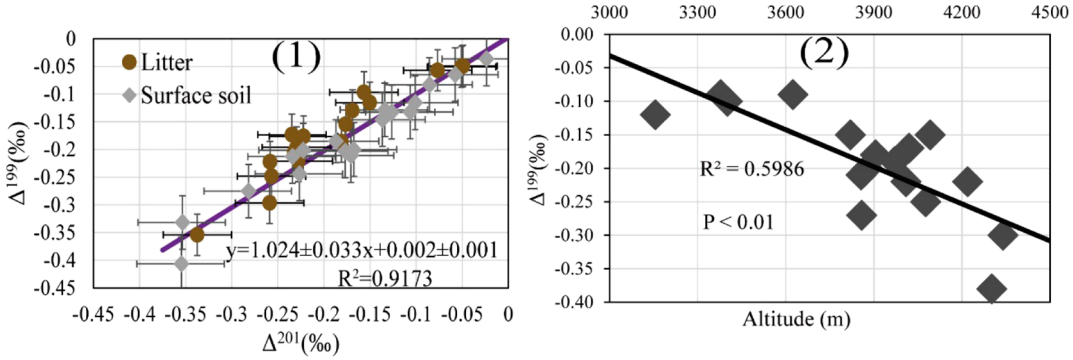

Figure 3. (1) Mass-independent fractionations Δ^{199}Hg (mean ± SD) vs Δ^{201}Hg (mean ± SD) in litter and surface soil samples and (2) Δ^{199}Hg in litter vs altitude. The Williamson−Yor- type regression deployed for (1) considers uncertainties of measurements, and detailed information can be found in an earlier report.[90]

that both wet and dry Hg depositions in the TP region can be up to 1 order of magnitude smaller than those in other forest sites in China, North America, and Europe (Figure 2.4,5). At the sites where low Hg dry deposition was observed, one important cause is the relatively smaller forest productivity, which is 2−4 times lower than the average value for global forests.[55]

3.2. Hg Isotopic Composition in Litter. As shown in Table S1, litter δ^{202}Hg ranges from −3.53 to −2.38‰ (mean = −2.93 ± 0.32‰, n = 17), and the range of litter Δ^{199}Hg is −0.38 to −0.05‰ (mean = −0.18 ± 0.09‰, n = 15). The litter δ^{202}Hg values are relatively more negative than those reported for the coniferous litter of North America and Europe (−2.78 to −1.34‰, mean = −1.99 ± 0.55‰, n = 9)[23,25] but comparable to the values observed at a high mountain site in China (Mt. Ailao) with an elevation of 2600 m (−2.43 to −4.18‰, mean = −3.03 ± 0.28‰, n = 73).[56] Such Δ^{199}Hg values are comparable to the findings in a deciduous forest in northern Wisconsin, USA (Δ^{199}Hg: −0.22 to −0.15‰, mean = −0.21 ± 0.07‰, n = 5)[23] and a coniferous forest at a mountain site in Eastern China (Mt. Daomei) (Δ^{199}Hg: −0.02 to −0.37‰, mean = −0.22 ± 0.10‰, n = 11)[56] but relatively less negative than those found in a Fennoscandia boreal coniferous forest (Δ^{199}Hg: −0.48 to −0.40‰, mean = −0.44 ± 0.02‰, n = 4)[25] and at the sites of Mt. Ailao (Δ^{199}Hg: −0.62 to −0.17‰, mean = −0.40 ± 0.08‰, n = 73).[56]

Atmospheric air samples at background sites show δ^{202}Hg values ranging from −0.35 to 1.19‰, much higher than those reported for litter samples (−1.64 to −4.18‰) at the same sites.[20,22,23,56] This can be explained by the Hg MDF during uptake of atmospheric Hg by plants. Lighter Hg isotopes in air can be preferentially accumulated in the foliage, leading to a shift from −3.0 to −1.0‰ in foliage δ^{202}Hg.[23,27,56]

The Δ^{199}Hg versus Δ^{201}Hg scatter plot for litter samples yields a slope of ∼1 (Figure 3.1), consistent with the observed slope caused by photoreduction of aqueous Hg^{II} showing a magnetic isotope effect (MIE).[20,57,58] Atmospheric Hg shows negative MIF with a Δ^{199}Hg:Δ^{201}Hg ratio of ∼1.[23,26,56,59] Litter MIF is mainly inherited from atmospheric Hg,[23,26,27,56] although recent studies have demonstrated that re-emission of Hg in the foliage can shift the litter Δ^{199}Hg by −0.1 to −0.05‰.[23,56] In our study, litter Δ^{199}Hg decreases with increasing altitude (Figure 3.2), and re-emission of Hg in the foliage cannot fully explain the large variation of Δ^{199}Hg from 3100 (−0.05‰) to 4300 m (−0.38‰).

Another hypothesis for the smaller Δ^{199}Hg (−0.12 to −0.05‰) at lower altitudes (3100−3600 m) is the adsorption of a greater quantity of particulate-bound Hg (PBM) on the litter surface, since PBM at background sites has positive Δ^{199}Hg values (0.48 ± 0.35‰, n = 10),[60] and the mixing of PBM and gaseous Hg^0 in the litter could lead to more positive Δ^{199}Hg at lower altitudes. However, the PBM absorbed at the foliage surface tends to be released through photochemical reduction or washed off by precipitation, and thus, PBM accounts for a small fraction of the total Hg in foliage.[61−64]

The most likely reason for the observed Hg isotopic composition is the stronger influence of anthropogenic Hg at lower altitudes, as Hg directly emitted from anthropogenic sources has been shown with Δ^{199}Hg ∼ 0.[20,24,56,65] Recent studies have suggested a sharp decrease in the anthropogenic Hg contribution from low to high altitudes of the eastern TP.[10] As shown in Figure S2, higher population densities occur at the low altitude sites of the study area and therefore have a greater influence of anthropogenic Hg emissions. Mountains in the eastern TP have led to relatively poor air diffusion at lower altitudes than higher altitudes.[66] The more negative Δ^{199}Hg (−0.38 to −0.15‰) in litter at high-altitude sites (3700−4300 m) possibly reflects long-range transport of atmospheric Hg, which has a stronger negative Δ^{199}Hg than anthropogenic Hg sources. Samples of high-elevation mountain glaciers, snow, and ice also point to Hg from long-range transport as the main sources.[9,67,68]

The relationship between Hg concentrations and Hg isotopes is provided in Figure S3. Higher litter Hg concentrations did not occur at lower altitudes (Figure S3.1), and a strong correlation between Δ^{199}Hg and the Hg concentration was not identified (Figure S3.2). It is likely that in addition to the atmospheric Hg concentration, tree species, leaf age, and leaf mass can also influence Hg accumulation in foliage.[62,69,70] An earlier study in the TP suggested the longer leaf lifespan at higher elevations, for instance, 10.4 years for *Picea crassifolia* at 2750 m versus 13.2 years at 3350 m.[71] A longer leaf lifespan leads to extended foliage exposure to atmospheric Hg.[5,72] Therefore, litter Δ^{199}Hg does not have to be correlated to litter Hg concentrations.

3.4. Hg Isotopic Composition in Soil. δ^{202}Hg and Δ^{199}Hg values of surface soil range from −2.98 to −0.69‰ (mean = −1.56 ± 0.54‰, n = 21) and from −0.46 to −0.04‰ (mean = −0.19 ± 0.12‰, n = 21), respectively (Table S1). The Δ^{199}Hg values are comparable to earlier observations on the forest floor

DOI: 10.1021/acs.est.6b03806
Environ. Sci. Technol. 2017, 51, 801−809

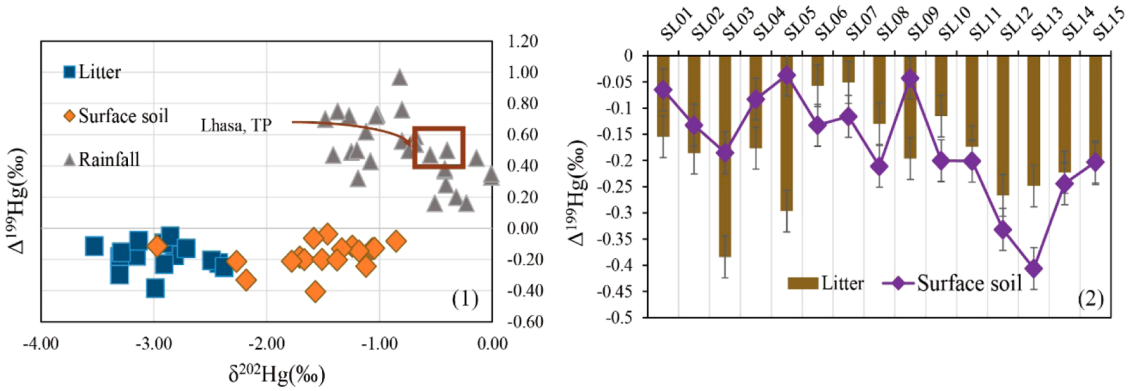

Figure 4. (1) Δ^{199}Hg vs δ^{202}Hg for precipitation, litter, and surface soil samples and (2) Δ^{199}Hg in litter and in surface soil for each sampling site. The Hg isotope composition in precipitation (≤10 ng L^{-1}) is derived from the literature.[23,74,79−81]

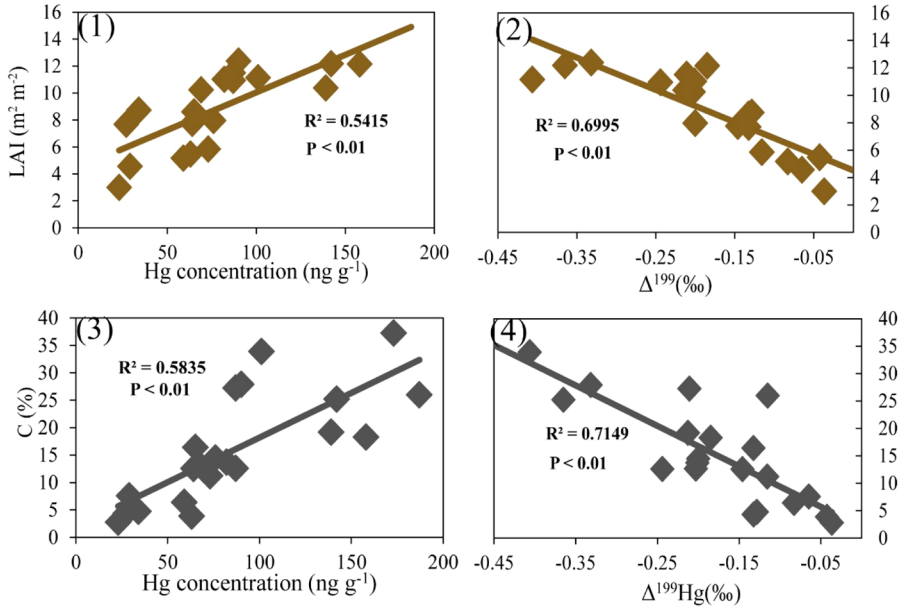

Figure 5. (1) Leaf area index vs Hg concentration in surface soil. (2) Leaf area index vs Δ^{199}Hg in surface soil. (3) C content in surface soil vs Hg concentration in surface soil. (4) C content in surface soil vs Δ^{199}Hg in surface soil.

elsewhere (−0.48 to −0.18‰, mean = −0.35 ± 0.08‰, n = 15).[23,25,73] The 30−60 cm soil has a much smaller Δ^{199}Hg (−0.06 ± 0.02‰ for the SL01, S002, and SL10 sites; Table S2) compared with surface soil. In addition, the mean δ^{202}Hg in 30−60 cm soil is −1.39 ± 0.17‰ (Table S2).

Hg in surface forest soil is mainly contributed from precipitation, litter, and weathered rocks. Surface soil has a more positive δ^{202}Hg than litter (P = 0.00; Figure S3) and a more negative δ^{202}Hg than precipitation (−0.80 to 0.40 ‰, mean = 0.60 ± 0.15‰, P = 0.00, n = 4).[74] Variations of soil δ^{202}Hg can be explained by the mixing of Hg input sources and postdepositional processes that fractionate Hg isotopes. Evasion of soil Hg through biotic reduction followed by volatilization has been shown to induce MDF but no MIF of Hg isotopes.[20,22,75]

There are two possible pathways that can induce the MIF of postdeposited Hg: one is photoreduction of soil Hg, which is associated with the MIE (Δ^{199}Hg:Δ^{201}Hg ∼ 1); the other is dark reduction by natural organic matter, which is associated with the nuclear volume effect (NVE) (Δ^{199}Hg:Δ^{201}Hg ∼ 1.6).[20,23,25] The dense canopy shading in forest ecosystems largely limits photoreduction of soil Hg.[76−78] An earlier study in northern Wisconsin forests suggested that photoreduction mainly occurred on leaf surfaces but not in soil.[23] A recent study in a boreal coniferous forest in northern Europe demonstrated that NVE can occur in histosol soils, but this effect seems to be limited.[25] In this study, the Δ^{199}Hg:Δ^{201}Hg ratio of ∼1 for the TP soils is consistent with that of litterfall (Figure 3.1) and in precipitation,[74] indicating that soil MIF is mainly inherited from atmospheric inputs and that postdepositional processes play a less important role in changing soil MIF signatures.

Figure 4 shows that except for the sites SL01, SL04, SL05, and SL09, the Δ^{199}Hg values in the surface soil (−0.37 to −0.13‰, mean = −0.23 ± 0.10‰) are more consistent with the Δ^{199}Hg in litter (−0.38 to −0.09‰, mean = −0.20 ± 0.08‰; t test, P = 0.61) than the Δ^{199}Hg of −0.06 ± 0.02‰ in 30−60 cm soil and the positive Δ^{199}Hg in the precipitation of the TP (0.35‰ to 0.75‰).[74] In addition, the litter and surface soil both have Δ^{200}Hg close to 0 (Table S1). Such Δ^{200}Hg values are distinctively different from the values in precipitation in the TP (0.10 to 0.16‰).[74] These results suggest that Hg deposition through litterfall dominates Hg accumulation in soil at these sites. Earlier studies reported negative Δ^{199}Hg in soil

DOI: 10.1021/acs.est.6b03806
Environ. Sci. Technol. 2017, 51, 801−809

from North American and European forests, which has been explained by litter contribution (80−90%).[23,25,26]

For deep soil and soil at sites SL01, SL04, SL05, and SL09, we observed less negative Δ^{199}Hg values ranging from −0.10 to 0‰ (Table S2). This may be explained by dilution of MIF by other Hg sources such as Hg wet deposition (with positive MIF)[23,74,79−81] and weathering of rocks (with no MIF).[24] Hg deposition through litterfall dominates the atmospheric Hg inputs at most sites in the TP. However, in contrast to the Δ^{199}Hg in litter, we did not observe an elevation gradient for Δ^{199}Hg in surface soil (R^2 = 0.02, P = 0.90). Earlier studies have suggested that litter biomass production can play a more important role than the Hg concentration in controlling the Hg deposition from litterfall at elevated mountain forests sites.[82−84] Therefore, one hypothesis is that the litter biomass production in the TP does not exhibit an elevation gradient because of the complicated orographic impacts.

The C content in the surface soil (Table S2) comes from decomposition of litter. Adaptation of plants to local climate causes the LAI (Table S2) to be closely coupled with net primary productivity,[85,86] and a higher LAI implies greater litter biomass production. We observed a clear correlation between C content and LAI (R = 0.77, P = 0.00). Figure 5 shows that higher C content and LAI are both associated with higher Hg concentrations as well as more negative Δ^{199}Hg. This suggests the important role of litter biomass production in atmospheric Hg inputs. Furthermore, poor correlations of altitude with LAI (R^2 = 0.04, P = 0.78) and C content (R^2 = 0.01, P = 1.02) verify the above hypothesis. This is consistent with the results from earlier surveys at about 100 forest sampling sites in the TP.[30,31]

The Δ^{199}Hg in litter ($\Delta^{199}Hg_L$, in ‰), soil C content (in %), and LAI (in m^2 m^{-2}) can be utilized to estimate the Δ^{199}Hg in surface soil of the TP ($\Delta^{199}Hg_S$, in ‰) with an empirical (regression) model (R^2 = 0.95):

$$\Delta^{199}Hg_S = 0.3524 - 0.0855 \times LAI + 0.0027 \times C + 0.9169 \times \Delta^{199}Hg_L + 0.0018 \times LAI \times C - 0.2934 \times LAI \times \Delta^{199}Hg_L + 0.1335 \times C \times \Delta^{199}Hg_L \quad (6)$$

4. ENVIRONMENTAL IMPLICATIONS

Earlier mass balance studies have highlighted that Hg deposition caused by the "cold trapping" effect is the dominant deposition pathway for Hg accumulation in surface soil in elevated montane regions.[5,72,87,88] The cold trapping effect is the preferential accumulation of Hg under the lower temperature at higher elevations,[5,72,87,88] which shifts predominant Hg input from litter in low-elevation forests to precipitation in high-elevation forests.[5,72,87,88]

Zhang et al.[6] reported dramatic variations in Hg concentrations and isotopic compositions in surface soil collected from a mountain gradient at Mt. Leigong in southwest China,[6] where enhanced Hg accumulation in the soil was observed at higher elevations, caused by a combination of higher litterfall Hg influx, higher precipitation rate, and mountain cold trapping effect-related wet deposition. Negative MIF was observed in the surface soil samples, with more negative MIF at higher elevations.[6] On the basis of the results in this and other studies,[23,25,56] Hg in litterfall is characterized with negative MIF and is likely the main source of MIF in the soil samples of Mt. Leigong. The less negative MIF at lower altitudes can be explained by dilution of geogenic sources with no MIF or the nearby anthropogenic Hg source in that area with relatively positive MIF.[6] This is consistent with the observations of our study that Hg input from litterfall dominates the Hg accumulation on the TP forest floor.

Litter biomass production has been well-documented through observations at ∼100 forest sites in the TP.[30,31] On the basis of meteorological data from 36 nearby weather stations, precipitation (R^2 = 0.88, P = 0.00) and temperature (R^2 = 0.87, P = 0.00) are the primary causes for litter biomass production in the TP.[30,31] Therefore, the cold-trapping-related precipitation and temperature in the TP likely have an indirect effect on Hg accumulation in surface soil by influencing the litter biomass production. A recent study also suggested that soil Hg concretion in the western United States is controlled by the water-limited plant primary productivity.[89] This is consistent with our results in the TP. Overall, this study provides new insights in understanding Hg accumulation in montane forested areas.

■ ASSOCIATED CONTENT

Supporting Information

The Supporting Information is available free of charge on the ACS Publications website at DOI: 10.1021/acs.est.6b03806.

Sample pretreating and measurements, Tables S1 and S2, and Figures S1−S4 (PDF)

■ AUTHOR INFORMATION

Corresponding Author

*Phone: +86-851-5895728; e-mail: fengxinbin@vip.skleg.cn.

ORCID

Xinbin Feng: 0000-0002-7462-8998

Notes

The authors declare no competing financial interest.

■ ACKNOWLEDGMENTS

This work was funded by the National 973 Program of China (2013CB430003) and the National Natural Science Foundation of China (41303014 and 41471416). We thank Mei Lu, Xia Jicheng, and Zhu Zhongqiang for assistance with sample measurements.

■ REFERENCES

(1) Agnan, Y.; Le Dantec, T.; Moore, C. W.; Edwards, G. C.; Obrist, D. New Constraints on Terrestrial Surface−Atmosphere Fluxes of Gaseous Elemental Mercury Using a Global Database. *Environ. Sci. Technol.* **2016**, *50* (2), 507−524.

(2) Lindberg, S. E.; Bullock, R.; Ebinghaus, R.; Engstrom, D.; Feng, X. B.; Fitzgerald, W.; Pirrone, N.; Prestbo, E.; Seigneur, C. A synthesis of progress and uncertainties in attributing the sources of mercury in deposition. *Ambio* **2007**, *36* (1), 19−32.

(3) Gustin, M. S.; Lindberg, S. E.; Weisberg, P. J. An update on the natural sources and sinks of atmospheric mercury. *Appl. Geochem.* **2008**, *23* (3), 482−493.

(4) Chang, R. Y.; Wang, G. X.; Fei, R.; Yang, Y.; Luo, J.; Fan, J. R. Altitudinal Change in Distribution of Soil Carbon and Nitrogen in Tibetan Montane Forests. *Soil Sci. Soc. Am. J.* **2015**, *79* (5), 1455−1469.

(5) Blackwell, B. D.; Driscoll, C. T. Deposition of Mercury in Forests along a Montane Elevation Gradient. *Environ. Sci. Technol.* **2015**, *49* (9), 5363−5370.

DOI: 10.1021/acs.est.6b03806
Environ. Sci. Technol. 2017, 51, 801−809

(6) Zhang, H.; Yin, R. S.; Feng, X. B.; Sommar, J.; Anderson, C. W. N.; Sapkota, A.; Fu, X. W.; Larssen, T. Atmospheric mercury inputs in montane soils increase with elevation: evidence from mercury isotope signatures. *Sci. Rep.* **2013**, *3*, 3322.
(7) Townsend, J. M.; Driscoll, C. T.; Rimmer, C. C.; McFarland, K. P. Avian, Salamander and, Forest Floor Mercury Concentrations Increase with Elevation in a Terrestrial Ecosystem. *Environ. Toxicol. Chem.* **2014**, *33* (1), 208−215.
(8) Yin, R. S.; Feng, X. B.; Hurley, J. P.; Krabbenhoft, D. P.; Lepak, R. F.; Kang, S. C.; Yang, H. D.; Li, X. D. Historical Records of Mercury Stable Isotopes in Sediments of Tibetan Lakes. *Sci. Rep.* **2016**, *6*, 23332.
(9) Loewen, M.; Kang, S.; Armstrong, D.; Zhang, Q.; Tomy, G.; Wang, F. Atmospheric transport of mercury to the Tibetan plateau. *Environ. Sci. Technol.* **2007**, *41* (22), 7632−7638.
(10) Gong, P.; Wang, X. P.; Xue, Y. G.; Xu, B. Q.; Yao, T. D. Mercury distribution in the foliage and soil profiles of the Tibetan forest: Processes and implications for regional cycling. *Environ. Pollut.* **2014**, *188*, 94−101.
(11) Huang, J.; Kang, S. C.; Zhang, Q. G.; Yan, H. Y.; Guo, J. M.; Jenkins, M. G.; Zhang, G. S.; Wang, K. Wet deposition of mercury at a remote site in the Tibetan Plateau: Concentrations, speciation,and fluxes. *Atmos. Environ.* **2012**, *62*, 540−550.
(12) Luo, J.; She, J.; Yang, P. J.; Sun, S. Q.; Li, W.; Gong, Y. W.; Tang, R. G. Heavy metal concentrations in timberline trees of eastern Tibetan Plateau. *Ecotoxicology* **2014**, *23* (6), 1086−1098.
(13) Tang, R.; Wang, H.; Luo, J.; Sun, S.; Gong, Y.; She, J.; Chen, Y.; Dandan, Y.; Zhou, J. Spatial distribution and temporal trends of mercury and arsenic in remote timberline coniferous forests, eastern of the Tibet Plateau, China. *Environ. Sci. Pollut. Res.* **2015**, *22* (15), 11658−11668.
(14) Allan, C. J.; Heyes, A.; Roulet, N. T.; St. Louis, V. L.; Rudd, J. W. M. Spatial and temporal dynamics of mercury in Precambrian Shield upland runoff. *Biogeochemistry* **2001**, *52* (1), 13−40.
(15) Carpi, A.; Lindberg, S. E.; Prestbo, E. M.; Bloom, N. S. Methyl mercury contamination and emission to the atmosphere from soil amended with municipal sewage sludge. *J. Environ. Qual* **1997**, *26* (6), 1650−1655.
(16) Xu, X.; Zhang, Q.; Wang, W.-X. Linking mercury, carbon, and nitrogen stable isotopes in Tibetan biota: Implications for using mercury stable isotopes as source tracers. *Sci. Rep.* **2016**, *6*, 25394.
(17) Li, C. D.; Zhang, Q. G.; Kang, S. C.; Liu, Y. Q.; Huang, J.; Liu, X. B.; Guo, J. M.; Wang, K.; Cong, Z. Y. Distribution and enrichment of mercury in Tibetan lake waters and their relations with the natural environment. *Environ. Sci. Pollut. Res.* **2015**, *22* (16), 12490−12500.
(18) Zhang, Q. G.; Pan, K.; Kang, S. C.; Zhu, A. J.; Wang, W. X. Mercury in Wild Fish from High-Altitude Aquatic Ecosystems in the Tibetan Plateau. *Environ. Sci. Technol.* **2014**, *48* (9), 5220−5228.
(19) Blum, J. D.; Bergquist, B. A. Reporting of variations in the natural isotopic composition of mercury. *Anal. Bioanal. Chem.* **2007**, *388* (2), 353−359.
(20) Blum, J. D.; Sherman, L. S.; Johnson, M. W. Mercury Isotopes in Earth and Environmental Sciences. *Annu. Rev. Earth Planet. Sci.* **2014**, *42*, 249−269.
(21) Sonke, J. E.; Blum, J. D. Advances in mercury stable isotope biogeochemistry Preface. *Chem. Geol.* **2013**, *336*, 1−4.
(22) Yin, R.; Feng, X.; Li, X.; Yu, B.; Du, B. Trends and advances in mercury stable isotopes as a geochemical tracer. *Trends Environ. Anal. Chem.* **2014**, *2*, 1−10.
(23) Demers, J. D.; Blum, J. D.; Zak, D. R. Mercury isotopes in a forested ecosystem: Implications for air-surface exchange dynamics and the global mercury cycle. *Global Biogeochem Cy* **2013**, *27* (1), 222−238.
(24) Yin, R. S.; Feng, X. B.; Shi, W. F. Application of the stable-isotope system to the study of sources and fate of Hg in the environment: A review. *Appl. Geochem.* **2010**, *25* (10), 1467−1477.
(25) Jiskra, M.; Wiederhold, J. G.; Skyllberg, U.; Kronberg, R. M.; Hajdas, I.; Kretzschmar, R. Mercury Deposition and Re-emission Pathways in Boreal Forest Soils Investigated with Hg Isotope Signatures. *Environ. Sci. Technol.* **2015**, *49* (12), 7188−7196.
(26) Enrico, M.; Le Roux, G.; Marusczak, N.; Heimburger, L. E.; Claustres, A.; Fu, X. W.; Sun, R. Y.; Sonke, J. E. Atmospheric Mercury Transfer to Peat Bogs Dominated by Gaseous Elemental Mercury Dry Deposition. *Environ. Sci. Technol.* **2016**, *50* (5), 2405−2412.
(27) Yin, R. S.; Feng, X. B.; Meng, B. Stable Mercury Isotope Variation in Rice Plants (Oryza sativa L.) from the Wanshan Mercury Mining District, SW China. *Environ. Sci. Technol.* **2013**, *47* (5), 2238−2245.
(28) Tang, R. G.; Luo, J.; She, J.; Chen, Y. C.; Yang, D. D.; Zhou, J. The cadmium and lead of soil in timberline coniferous forests, Eastern Tibetan Plateau. *Environ. Earth Sci.* **2015**, *73* (1), 303−310.
(29) Luo, J.; She, J.; Wu, Y. H.; Yu, D.; Chen, Y. C.; Zhou, P. Cadmium Distribution in a Timberline Forest in the Hengduan Mountains in the Eastern Tibetan Plateau. *Anal. Lett.* **2013**, *46* (2), 394−405.
(30) Wang, G. X.; Ran, F.; Chang, R. Y.; Yang, Y.; Luo, J.; Fan, J. R. Variations in the live biomass and carbon pools of Abies georgei along an elevation gradient on the Tibetan Plateau, China. *For. Ecol. Manage.* **2014**, *329*, 255−263.
(31) Yang, Y.; Wang, G.; Ran, F.; Chang, R. Litter carbon stock and spatial patterns of main forest types in Tibet. *Chin. J. Ecol* **2016**, *35* (3), 559−566.
(32) Fang, H.; Li, W.; Wei, S.; Jiang, C. Corrigendum to "Seasonal variation of leaf area index (LAI) over paddy rice fields in NE China: Intercomparison of destructive sampling, LAI-2200, digital hemispherical photography (DHP), and AccuPAR methods" Agricultural and Forest Meteorology, Volume 198-199(2014), 126-41. *Agric. For. Meteorol.* **2015**, *214-215*, 1.
(33) Zhou, J.; Feng, X. B.; Liu, H. Y.; Zhang, H.; Fu, X. W.; Bao, Z. D.; Wang, X.; Zhang, Y. P. Examination of total mercury inputs by precipitation and litterfall in a remote upland forest of Southwestern China. *Atmos. Environ.* **2013**, *81*, 364−372.
(34) Maynard, D.; Curran, M. Bulk density measurement in forest soils. In *Soil Sampling and Methods of Analysis*, 2nd ed.; CRC Press: Boca Raton, FL, 2007.
(35) Sun, R. Y.; Heimburger, L. E.; Sonke, J. E.; Liu, G. J.; Amouroux, D.; Berail, S. Mercury stable isotope fractionation in six utility boilers of two large coal-fired power plants. *Chem. Geol.* **2013**, *336*, 103−111.
(36) Estrade, N.; Carignan, J.; Sonke, J. E.; Donard, O. F. X. Measuring Hg Isotopes in Bio-Geo-Environmental Reference Materials. *Geostand. Geoanal. Res.* **2010**, *34* (1), 79−93.
(37) Ma, M.; Wang, D.; Du, H.; Sun, T.; Zhao, Z.; Wang, Y.; Wei, S. Mercury dynamics and mass balance in a subtropical forest, southwestern China. *Atmos. Chem. Phys. Discuss.* **2015**, *15* (24), 35857−35880.
(38) Ma, M.; Wang, D. Y.; Du, H. X.; Sun, T.; Zhao, Z.; Wei, S. Q. Atmospheric mercury deposition and its contribution of the regional atmospheric transport to mercury pollution at a national forest nature reserve, southwest China. *Environ. Sci. Pollut. Res.* **2015**, *22* (24), 20007−20018.
(39) Wang, Z. W.; Zhang, X. S.; Xiao, J. S.; Zhijia, C.; Yu, P. Z. Mercury fluxes and pools in three subtropical forested catchments, southwest China. *Environ. Pollut.* **2009**, *157* (3), 801−808.
(40) Zhou, J.; Wang, Z. W.; Zhang, X. S.; Chen, J. Distribution and elevated soil pools of mercury in an acidic subtropical forest of southwestern China. *Environ. Pollut.* **2015**, *202*, 187−195.
(41) Choi, H. D.; Holsen, T. M.; Hopke, P. K. Atmospheric mercury (Hg) in the Adirondacks: Concentrations and sources. *Environ. Sci. Technol.* **2008**, *42* (15), 5644−5653.
(42) Demers, J. D.; Driscoll, C. T.; Fahey, T. J.; Yavitt, J. B. Mercury cycling in litter and soil in different forest types in the Adirondack region, New York, USA. *Ecol Appl.* **2007**, *17* (5), 1341−1351.
(43) Larssen, T.; de Wit, H. A.; Wiker, M.; Halse, K. Mercury budget of a small forested boreal catchment in southeast Norway. *Sci. Total Environ.* **2008**, *404* (2−3), 290−296.

DOI: 10.1021/acs.est.6b03806
Environ. Sci. Technol. 2017, 51, 801−809

(44) Mason, R. P.; Lawson, N. M.; Sheu, G. R. Annual and seasonal trends in mercury deposition in Maryland. *Atmos. Environ.* **2000**, *34* (11), 1691−1701.
(45) Schwesig, D.; Matzner, E. Pools and fluxes of mercury and methylmercury in two forested catchments in Germany. *Sci. Total Environ.* **2000**, *260* (1−3), 213−223.
(46) St. Louis, V. L.; Rudd, J. W. M.; Kelly, C. A.; Hall, B. D.; Rolfhus, K. R.; Scott, K. J.; Lindberg, S. E.; Dong, W. Importance of the forest canopy to fluxes of methyl mercury and total mercury to boreal ecosystems. *Environ. Sci. Technol.* **2001**, *35* (15), 3089−3098.
(47) Fu, X. W.; Feng, X.; Dong, Z. Q.; Yin, R. S.; Wang, J. X.; Yang, Z. R.; Zhang, H. Atmospheric gaseous elemental mercury (GEM) concentrations and mercury depositions at a high-altitude mountain peak in south China. *Atmos. Chem. Phys.* **2010**, *10* (5), 2425−2437.
(48) Luo, Y.; Duan, L.; Wang, L.; Xu, G. Y.; Wang, S. X.; Hao, J. M. Mercury concentrations in forest soils and stream waters in northeast and south China. *Sci. Total Environ.* **2014**, *496*, 714−720.
(49) Navratil, T.; Shanley, J.; Rohovec, J.; Hojdova, M.; Penizek, V.; Buchtova, J. Distribution and Pools of Mercury in Czech Forest Soils. *Water, Air, Soil Pollut.* **2014**, *225* (3), 1829.
(50) Obrist, D.; Johnson, D. W.; Lindberg, S. E.; Luo, Y.; Hararuk, O.; Bracho, R.; Battles, J. J.; Dail, D. B.; Edmonds, R. L.; Monson, R. K.; Ollinger, S. V.; Pallardy, S. G.; Pregitzer, K. S.; Todd, D. E. Mercury Distribution Across 14 US Forests. Part I: Spatial Patterns of Concentrations in Biomass, Litter, and Soils. *Environ. Sci. Technol.* **2011**, *45* (9), 3974−3981.
(51) Huang, J.; Kang, S. C.; Wang, S. X.; Wang, L.; Zhang, Q. G.; Guo, J. M.; Wang, K.; Zhang, G. S.; Tripathee, L. Wet deposition of mercury at Lhasa, the capital city of Tibet. *Sci. Total Environ.* **2013**, *447*, 123−132.
(52) Huang, J.; Kang, S. C.; Zhang, Q. G.; Guo, J. M.; Sillanpaa, M.; Wang, Y. J.; Sun, S. W.; Sun, X. J.; Tripathee, L. Characterizations of wet mercury deposition on a remote high-elevation site in the southeastern Tibetan Plateau. *Environ. Pollut.* **2015**, *206*, 518−526.
(53) Huang, J.; Kang, S. C.; Zhang, Q. G.; Jenkins, M. G.; Guo, J. M.; Zhang, G. S.; Wang, K. Spatial distribution and magnification processes of mercury in snow from high-elevation glaciers in the Tibetan Plateau. *Atmos. Environ.* **2012**, *46*, 140−146.
(54) Grigal, D. F. Inputs and outputs of mercury from terrestrial watersheds: A review. *Environ. Rev.* **2002**, *10* (1), 1−39.
(55) Luo, T. X.; Li, W. H.; Zhu, H. Z. Estimated biomass and productivity of natural vegetation on the Tibetan Plateau. *Ecol Appl.* **2002**, *12* (4), 980−997.
(56) Yu, B.; Fu, X.; Yin, R.; Zhang, H.; Wang, X.; Lin, C.-J.; Wu, C.; Zhang, Y.; He, N.; Fu, P.; Wang, Z.; Shang, L.; Sommar, J.; Sonke, J. E.; Maurice, L.; Guinot, B.; Feng, X. Isotopic Composition of Atmospheric Mercury in China: New Evidence for Sources and Transformation Processes in Air and in Vegetation. *Environ. Sci. Technol.* **2016**, *50* (17), 9262−9.
(57) Bergquist, B. A.; Blum, J. D. Mass-dependent and -independent fractionation of Hg isotopes by photoreduction in aquatic systems. *Science* **2007**, *318* (5849), 417−420.
(58) Zheng, W.; Hintelmann, H. Mass independent isotope fractionation of mercury during its photochemical reduction by low-molecular-weight organic compounds. *Geochim. Cosmochim. Acta* **2010**, *74* (12 Suppl.), A1224.
(59) Fu, X.; Marusczak, N.; Wang, X.; Gheusi, F.; Sonke, J. E. Isotopic Composition of Gaseous Elemental Mercury in the Free Troposphere of the Pic du Midi Observatory, France. *Environ. Sci. Technol.* **2016**, *50* (11), 5641−5650.
(60) Rolison, J. M.; Landing, W. M.; Luke, W.; Cohen, M.; Salters, V. J. M. Isotopic composition of species-specific atmospheric Hg in a coastal environment. *Chem. Geol.* **2013**, *336*, 37−49.
(61) Graydon, J. A.; St. Louis, V. L.; Lindberg, S. E.; Hintelmann, H.; Krabbenhoft, D. P. Investigation of mercury exchange between forest canopy vegetation and the atmosphere using a new dynamic chamber. *Environ. Sci. Technol.* **2006**, *40* (15), 4680−4688.
(62) Laacouri, A.; Nater, E. A.; Kolka, R. K. Distribution and Uptake Dynamics of Mercury in Leaves of Common Deciduous Tree Species in Minnesota, U.S.A. *Environ. Sci. Technol.* **2013**, *47* (18), 10462−10470.
(63) Stamenkovic, J.; Gustin, M. S. Nonstomatal versus Stomatal Uptake of Atmospheric Mercury. *Environ. Sci. Technol.* **2009**, *43* (5), 1367−1372.
(64) Zhang, L.; Wright, L. P.; Blanchard, P. A review of current knowledge concerning dry deposition of atmospheric mercury. *Atmos. Environ.* **2009**, *43* (37), 5853−5864.
(65) Bessinger, B. A. Use of Stable Isotopes to Identify Sources of Mercury in Sediments: A Review and Uncertainty Analysis. *Environ. Forensics* **2014**, *15* (3), 265−280.
(66) Yanai, M.; Li, C. F. MECHANISM OF HEATING AND THE BOUNDARY-LAYER OVER THE TIBETAN PLATEAU. *Mon. Weather Rev.* **1994**, *122* (2), 305−323.
(67) Kang, S. C.; Huang, J.; Wang, F. Y.; Zhang, Q. G.; Zhang, Y. L.; Li, C. L.; Wang, L.; Chen, P. F.; Sharma, C. M.; Li, Q.; Sillanpaa, M.; Hou, J. Z.; Xu, B. Q.; Guo, J. M. Atmospheric Mercury Depositional Chronology Reconstructed from Lake Sediments and Ice Core in the Himalayas and Tibetan Plateau. *Environ. Sci. Technol.* **2016**, *50* (6), 2859−2869.
(68) Huang, J.; Kang, S. C.; Guo, J. M.; Sillanpaa, M.; Zhang, Q. G.; Qin, X.; Du, W. T.; Tripathee, L. Mercury distribution and variation on a high-elevation mountain glacier on the northern boundary of the Tibetan Plateau. *Atmos. Environ.* **2014**, *96*, 27−36.
(69) Ericksen, J. A.; Gustin, M. S.; Schorran, D. E.; Johnson, D. W.; Lindberg, S. E.; Coleman, J. S. Accumulation of atmospheric mercury in forest foliage. *Atmos. Environ.* **2003**, *37* (12), 1613−1622.
(70) Fostier, A. H.; Melendez-Perez, J. J.; Richter, L. Litter mercury deposition in the Amazonian rainforest. *Environ. Pollut.* **2015**, *206*, 605−610.
(71) Wu, Q.; Hu, Q.; Zheng, L.; Zhang, F.; Song, M.; Liu, X. Variations of Leaf Lifespan and Leaf Mass Per Area of Picea crassifolia along Altitude Gradient. *Acta Bot. Boreali-Occident. Sin.* **2010**, *30* (8), 1689−1694.
(72) Stankwitz, C.; Kaste, J. M.; Friedland, A. J. Threshold Increases in Soil Lead and Mercury from Tropospheric Deposition Across an Elevational Gradient. *Environ. Sci. Technol.* **2012**, *46* (15), 8061−8068.
(73) Tsui, M. T. K.; Blum, J. D.; Finlay, J. C.; Balogh, S. J.; Nollet, Y. H.; Palen, W. J.; Power, M. E. Variation in Terrestrial and Aquatic Sources of Methylmercury in Stream Predators as Revealed by Stable Mercury Isotopes. *Environ. Sci. Technol.* **2014**, *48* (17), 10128−10135.
(74) Yuan, S.; Zhang, Y.; Chen, J.; Kang, S.; Zhang, J.; Feng, X.; Cai, H.; Wang, Z.; Wang, Z.; Huang, Q., Large variation of mercury isotope composition during a single precipitation event at Lhasa City, Tibetan Plateau, China. In *11th Applied Isotope Geochemistry Conference AIG-11*; Millot, R., Negrel, P., Eds.; BRGM: Orléans, France, 2015; Vol. *13*, pp 282−286.
(75) Sonke, J. E. A global model of mass independent mercury stable isotope fractionation. *Geochim. Cosmochim. Acta* **2011**, *75* (16), 4577−4590.
(76) Carpi, A.; Lindberg, S. E. Application of a Teflon (TM) dynamic flux chamber for quantifying soil mercury flux: Tests and results over background soil. *Atmos. Environ.* **1998**, *32* (5), 873−882.
(77) Zhang, H.; Lindberg, S. E.; Gustin, M. S. Nature of diel trend of mercury emission from soil: Current understanding and hypotheses. *Abstr. Pap.—Am. Chem. Soc.* **2001**, *222*, U429.
(78) Choi, H. D.; Holsen, T. M. Gaseous mercury fluxes from the forest floor of the Adirondacks. *Environ. Pollut.* **2009**, *157* (2), 592−600.
(79) Gratz, L. E.; Keeler, G. J.; Blum, J. D.; Sherman, L. S. Isotopic Composition and Fractionation of Mercury in Great Lakes Precipitation and Ambient Air. *Environ. Sci. Technol.* **2010**, *44* (20), 7764−7770.
(80) Chen, J. B.; Hintelmann, H.; Feng, X. B.; Dimock, B. Unusual fractionation of both odd and even mercury isotopes in precipitation from Peterborough, ON, Canada. *Geochim. Cosmochim. Acta* **2012**, *90*, 33−46.
(81) Sherman, L. S.; Blum, J. D.; Keeler, G. J.; Demers, J. D.; Dvonch, J. T. Investigation of Local Mercury Deposition from a Coal-

DOI: 10.1021/acs.est.6b03806
Environ. Sci. Technol. 2017, 51, 801−809

Fired Power Plant Using Mercury Isotopes. *Environ. Sci. Technol.* **2012**, *46* (1), 382−390.
(82) Wang, X.; Bao, Z.; Lin, C.-J.; Yuan, W.; Feng, X. Assessment of global mercury deposition through litterfall. *Environ. Sci. Technol.* **2016**, *50*, 8548−8557.
(83) Fu, X. W.; Yang, X.; Lang, X. F.; Zhou, J.; Zhang, H.; Yu, B.; Yan, H. Y.; Lin, C. J.; Feng, X. B. Atmospheric wet and litterfall mercury deposition at urban and rural sites in China. *Atmos. Chem. Phys.* **2016**, *16* (18), 11547−11562.
(84) Wang, X.; Lin, C. J.; Lu, Z. Y.; Zhang, H.; Zhang, Y. P.; Feng, X. B. Enhanced accumulation and storage of mercury on subtropical evergreen forest floor: Implications on mercury budget in global forest ecosystems. *J. Geophys. Res.: Biogeosci.* **2016**, *121* (8), 2096−2109.
(85) Farquhar, G. D.; Ehleringer, J. R.; Hubick, K. T. Carbon Isotope Discrimination and Photosynthesis. *Annu. Rev. Plant Physiol. Plant Mol. Biol.* **1989**, *40*, 503−537.
(86) Luo, T. X.; Zhang, L.; Zhu, H. Z.; Daly, C.; Li, M. C.; Luo, J. Correlations between net primary productivity and foliar carbon isotope ratio across a Tibetan ecosystem transect. *Ecography* **2009**, *32* (3), 526−538.
(87) Lawson, S. T.; Scherbatskoy, T. D.; Malcolm, E. G.; Keeler, G. J. Cloud water and throughfall deposition of mercury and trace elements in a high elevation spruce-fir forest at Mt. Mansfield, Vermont. *J. Environ. Monit.* **2003**, *5* (4), 578−583.
(88) Huang, J. Y.; Gustin, M. S. Evidence for a Free Troposphere Source of Mercury in Wet Deposition in the Western United States. *Environ. Sci. Technol.* **2012**, *46* (12), 6621−6629.
(89) Obrist, D.; Pearson, C.; Webster, J.; Kane, T.; Lin, C. J.; Aiken, G. R.; Alpers, C. N. A synthesis of terrestrial mercury in the western United States: Spatial distribution defined by land cover and plant productivity. *Sci. Total Environ.* **2016**, *568*, 522−535.
(90) Cantrell, C. A. Technical Note: Review of methods for linear least-squares fitting of data and application to atmospheric chemistry problems. *Atmos. Chem. Phys.* **2008**, *8* (17), 5477−5487.

DOI: 10.1021/acs.est.6b03806
Environ. Sci. Technol. 2017, 51, 801−809